THE JOURNAL OF PHYSICAL CHEMISTRY B

Article

pubs.acs.org/JPCB

Measuring the Proton Conductivity of Ion-Exchange Membranes Using Electrochemical Impedance Spectroscopy and Through-Plane Cell

Franciélli Müller,[†] Carlos A. Ferreira,*[,†] Denise S. Azambuja,[‡] Carlos Alemán,[§,∥] and Elaine Armelin*[,§,∥]

[†]Departamento de Engenharia de Materiais, PPGEM, Universidade Federal do Rio Grande do Sul, Av. Bento Gonçalvez, 9500, Setor 4, Prédio 74 − 91501-970, Porto Alegre (Rio Grande do Sul), Brazil

[‡]Instituto de Química, Universidade Federal do Rio Grande do Sul, Av. Bento Gonçalves 9500 − CEP 91501-970, Porto Alegre (Rio Grande do Sul), Brazil

[§]Departament d'Enginyeria Química, ETSEIB, Universitat Politècnica de Catalunya, Av. Diagonal 647, 08028, Barcelona, Spain

[∥]Centre for Research in Nano-Engineering, Universitat Politècnica de Catalunya, Campus Sud, Edifici C', C/Pasqual i Vila s/n, 08028, Barcelona, Spain

Supporting Information

ABSTRACT: The role of the incorporation of conducting polymer (CP), doped with different sulfonic acid organic molecules, in polystyrene (PS) and high-impact polystyrene (HIPS) with poly(styrene-ethylene-butylene) (SEBS) triblock copolymer has been investigated. Two factors associated with this model membrane system are addressed: (i) the influence of the presence of a low concentration of doped conducting polymer and (ii) the influence of the membrane preparation method. Membrane characterization and bulk conductivity measurements allowed the conclusion that proton conductivity has been promoted by the addition of CP; the best results were achieved for PAni-CSA, in either PS/SEBS or HIPS/SEBS blends. Additionally, the water uptake only decreased with the addition of PAni-doped molecules compared to the pure copolymer, without loss of ion-exchange capacity (IEC). Electrodialysis efficiency for HIPS/SEBS (before annealing) is higher than that for HIPS/SEBS (after annealing), indicating that membrane preparation method is crucial. Finally, through-plane cell arrangement proved to be an effective, quick, and time-saving tool for studying the main resistance parameters of isolating polymers, which is useful for application in industry and research laboratories working with membranes for electrodialysis or fuel cells.

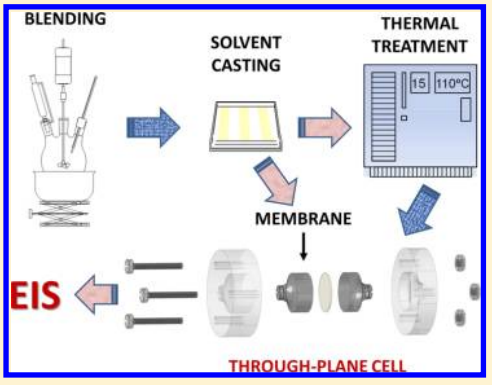

1. INTRODUCTION

Measurement of proton conductivity in isolating polymer films is a very complex task. Furthermore, results for a given polymer show a great dependence on a number of factors, such as film-casting conditions, relative humidity, cell configuration used to measure the film resistance, and pressure applied between probe electrodes.[1−7] Currently, the resistance of polymer films are frequently measured by the two-probe and four-probe methods using in-plane equipment construction. Accordingly, the proton conductivity can be determined along the plane of the film or across the film by applying through-plane cell geometry for measurements. Both procedures require the use of a potentiostat−galvanostat equipped with an impedance analyzer accessory or with a direct ac voltage amplifier sourcemeter.

Electrochemical impedance spectroscopy (EIS),[8] which is among the most powerful electrochemical techniques, can be also used to determine the solid-state polymer resistance, providing a straightforward way to estimate the conductivity of polymeric films. This technique enables the attainment of useful information about the interfacial double-layer capacitance (C_{dl}), polymer membrane bulk resistance (R_b), and polymer membrane bulk capacitance (C_b), which corresponds to the mobility of H^+ in the sulfonic acid groups ($-SO_3H$), bearing in mind that the electrolyte content is inside the polymer chain. In the present study we applied the through-plane impedance technique to evaluate the membrane bulk resistance of a series of block copolymers formed by amorphous sulfonated polystyrene copolymers (SPS), high-impact polystyrene (HIPS), and poly(styrene-ethylene-butylene) triblock copolymer (SEBS), which are employed as proton-exchange membranes for dialysis treatment.[9]

In a pioneering study, Holdcroft and co-workers[10] evaluated the proton conductivity of polymer membranes using in-plane and through-plane impedance techniques. The same authors concluded that the through-plane conductivity is the most

Received: September 27, 2013
Revised: December 20, 2013
Published: January 10, 2014

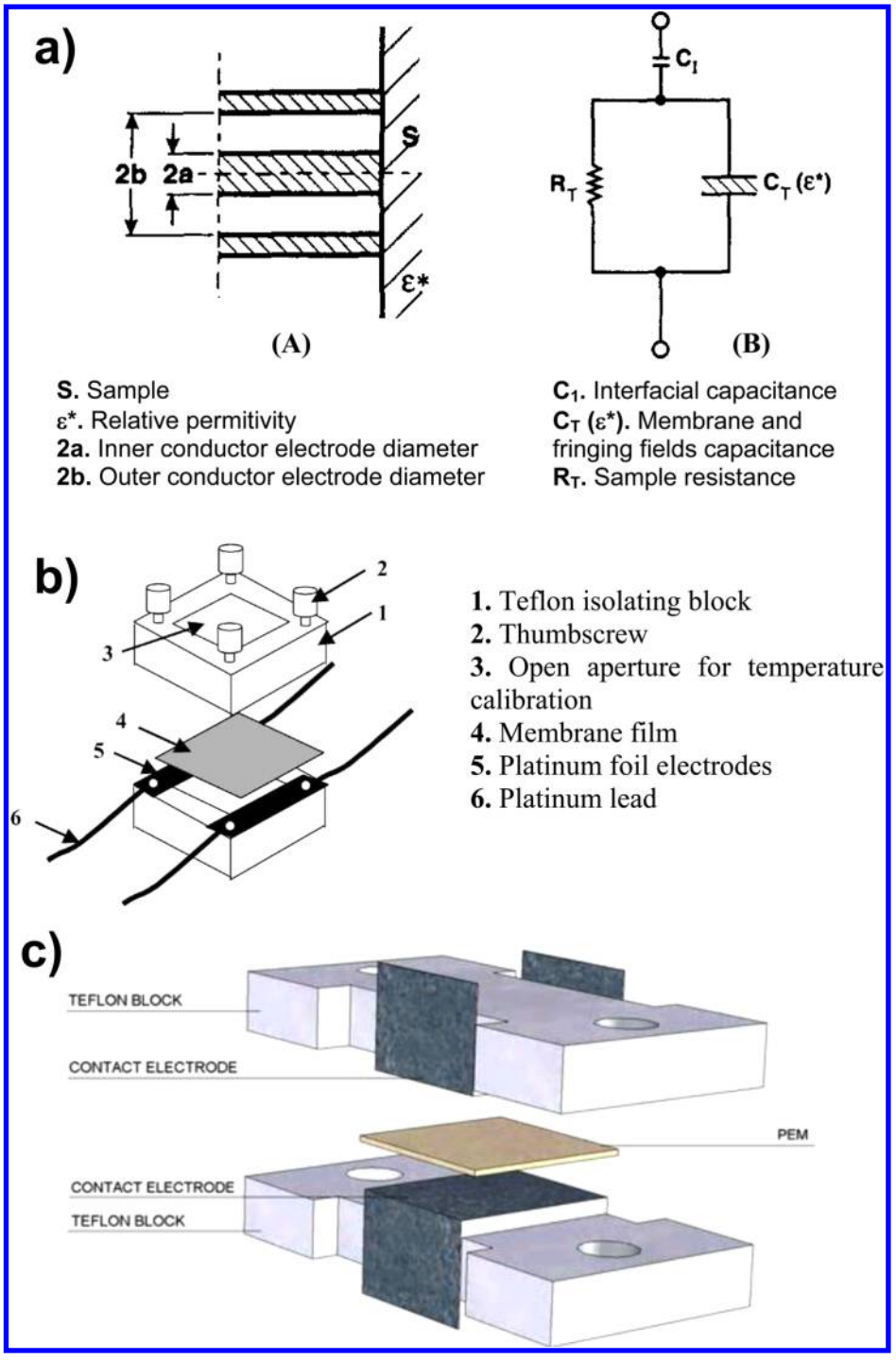

Figure 1. Some examples of cell geometries used for polymer films conductivity measurements. (a) A coaxial probe, where (A) represents the open-ended coaxial probe pressed against a sample of membrane and (B) the electrical equivalent circuit. (Reprinted with permission from ref 3. Copyright 1995 Elsevier.) (b) An in-plane cell configuration. (Reprinted with permission from ref 6. Copyright 2002 Elsevier.) (c) A through-plane cell probe arrangement, where PEM is the acronym of proton exchange membranes. (Reprinted with permission from ref 10. Copyright 2008 Elsevier.)

appropriate for fuel cell membranes because of the proton conduction requirements in the direction perpendicular to the membrane surface; these effects are specially remarkable when the material presents morphological anisotropy. After accurate calibration and fitting of the impedance spectra to the equivalent circuit, the anisotropy for the in-plane conductivity was found to be higher than that for the through-plane conductivity.[10] Furthermore, through-plane conductivity measurements were more reproducible than in-plane measurements for many of the assayed membranes.

On the other hand, several authors have reported the in-plane conductivity values for different classes of proton-exchange membranes (PEMs),[3,6,11−13] even though no standardized method was employed. Thus, bulk membrane resistances were determined using different cell geometries and configurations. Some examples of arrangements specially

dx.doi.org/10.1021/jp409675z | J. Phys. Chem. B 2014, 118, 1102−1112

designed for in-plane conductivity measurements are illustrated in Figure 1. A first approach was developed by Gardner and Anantaraman,[3] who used coaxial cell geometry to determine the membrane conductivity (Figure 1a). These authors postulated analytical expressions for small and larger coaxial probes, a strong dependence of the film resistance with the film thickness and the probe size being achieved. Coaxial probe was found to reduce the influence of external variables, such as humidity, while small probes allowed the measurment of local conductivities. McGrath and co-workers[6] reported another kind of conductivity cell geometry, which permitted the direct contact of the sample with the electrolyte solution (Figure 1b). On the other hand, there are few reports on the determination of the through-plane conductivity for PEMs.[5,7,9,14,15] The main handicap in such studies was to control all the external condition parameters that affect the conductivity values. On the basis of previous works,[16−24] Holdcroft and co-workers[10] designed a new cell geometry for through-plane method (Figure 1c) and described important details regarding good practice in measuring the membrane bulk resistance with good reproducibility.

Within this context, the proton conductivity of amorphous SPS, HIPS, and SEBS copolymers and their blends with conducting polymer (CP) have been evaluated. More specifically, this study is aimed at investigating the influence of sulfonation degree on the proton conductivity of these materials using an easy and improved through-plane conductivity method reported above.[10] Results have enabled the offering of new perspectives related to the conductivity measurements in dry and wet membrane systems. Furthermore, the effects of the addition of a small concentration of CP on the conductivity and stability of cation-exchange membranes (CEMs) have been also investigated. For this purpose, polyaniline (PAni) doped with camphorsulfonic acid (CSA), dodecylbenzenesulfonic acid (DBSA), or *p*-toluenesulfonic acid (TSA) have been used.

2. EXPERIMENTAL SECTION

2.1. Materials. PS (M_w = 27.5 × 10^3 g/mol) and HIPS (M_w = 16 × 10^3 g/mol) homopolymers were kindly supplied by Innova S.A. (PS-N2380 and HIPS-SR550). The SEBS, which was purchased from Kraton Co. (Catalog Number G-1650M), is a linear triblock copolymer with two PS end blocks (M_w = 10.3 × 10^3 g/mol) and a poly(ethylene-*co*-butylene) (PEB) midblock (M_w = 53.3 × 10^3 g/mol), both used in the preparation of the blends studied in this work. Aniline (Nuclear, ACS reagent, 99.9%), ammonium persulfate (Synth, reagent grade), hydrochloric acid (Sigma, ACS reagent, 37%), and ammonium hydroxide (Synth, ACS grade) were used for the synthesis of PAni emeraldine base. The resulting polymers were doped with CSA (Aldrich), DBSA (Lavrex), and TSA (Vetex).

2.2. Membrane Preparation and Characterization. Synthesis and physicochemical characterization of all partially sulfonated polymer blends were reported in our previous work.[25] The sulfonated PS/SEBS and HIPS/SEBS blends were diluted in dimethylformamide and poured on a glass plate, spread to uniform thickness (100−150 μm) with a spreader, and dried for 15 min at 110 °C in an oven. Compositions with CP were prepared considering 5 wt % of PAni doped with CSA, DBSA, or TSA (PAni-CSA, PAni-DBSA, and PAni-TSA, respectively). Synthesis of PAni-CSA was also reported in ref 25, and a similar procedure was employed to dope PAni with the other two acids. In the following, the labeling of blends modified with conducting polymer, for example PS/SEBS/PAni-CSA and HIPS/SEBS/PAni-CSA, refer to PS/SEBS and HIPS/SEBS, respectively, blended with PAni doped with CSA. A similar nomenclature has been used for the other two dopants, replacing CSA by DBSA or TSA.

The influence of the drying procedure on the bulk membrane resistance has been evaluated for HIPS/SEBS blends considering two different methods: (a) solvent casting at room temperature and (b) thermal treatment with films dried at 110 °C for 15 min in an oven and subsequently annealed overnight at 60 °C under vacuum. The membranes for all the other composition blends were prepared using procedure (b).

The water uptake (wt %) was determined by the mass difference between the wet and the dried membranes. Membranes were equilibrated in deionized water at room temperature for 24 h. The excess of water was removed with filter paper; then the membranes were weighed and kept in an oven at 80 °C for 12 h and then weighed again. Water absorption has been expressed in percent.

To determine the ion-exchange capacity (IEC), the membranes were equilibrated in 100 mL of 1 M HCl solution for 72 h. After that, they were removed from the solution, and the excess of acid was eliminated by washing with distilled water. Next, membranes were immersed in 1 M NaCl to exchange H^+ by Na^+; three renewed solutions were used in this process. The amount of H^+ in these three solutions was determined by titration with 0.005 M NaOH. The IEC was expressed in milliequivalents of H^+ per gram of dry membrane, according to eq 1.

$$\mathrm{IEC} = \frac{V_{\mathrm{NaOH}} M_{\mathrm{NaOH}}}{W_{\mathrm{dry}}} \tag{1}$$

where V_{NaOH} and M_{NaOH} are the blank-corrected volume (mL) and molar concentration (mol/L) of NaOH solution, respectively.

The degree of sulfonation (%) was measured according to the quantitative procedure indicated in the ASTM D5453-12.[26]

2.3. Conductivity Measurements. For a first screening, proton conductivity measurements were performed with dry membranes. The conductivity was determined by means of impedance measurements using an AutoLab PGSTAT302N frequency response analyzer (FRA) at AC amplitude of 10 mV. The frequency interval employed for the measurements ranged from 10kHz to 10mHz. Samples were sandwiched between two stainless steel disks (blocking electrodes composed by AISI 304 type), separated by a Teflon holder, corresponding to the through-plane conductivity homemade cell configuration shown in Figure 2. Although the cell used was described previously elsewhere,[27−30] here we give the exact cell dimensions and construction for research community reproducibility. The volume of the cell is defined by a 15 mm inner diameter and a 2 mm inner depth. The pressure is kept constant and defined by the maximum limits of screws used to close the probe arrangement. For the assays, the films were previously cut into disks (area = 1.766 cm^2); dry film thickness (DFT) values were measured with a Neurtek Mega-Check pocket FE device. Films were then painted on both sides with electrically conductivity silver paint (Diotronic S.A., catalogue reference Electrokit 3). This ensured a perfect contact between the film and the steel electrodes, avoiding impedance noise in

dx.doi.org/10.1021/jp409675z | J. Phys. Chem. B 2014, 118, 1102−1112

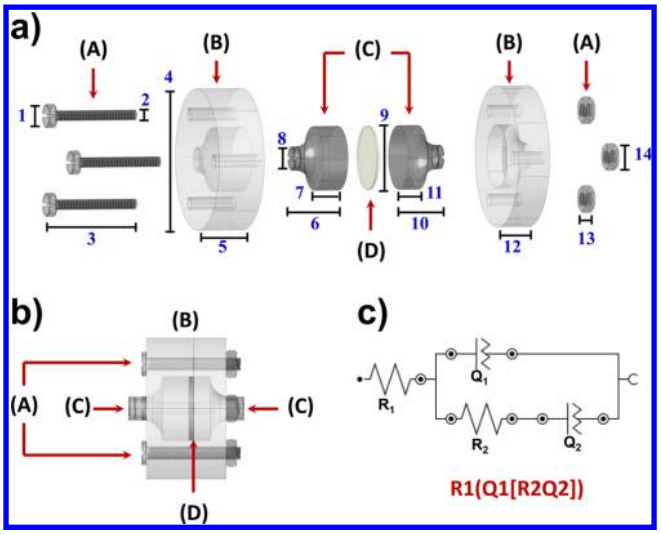

Figure 2. Schematic representation of the cell geometry and membrane arrangement used in the present study: (a) 3D open view of the individual parts of the through-plane impedance cell with their corresponding size (1, 5.40 mm; 2, 2.60 mm; 3, 22.10 mm; 4, 32.95 mm; 5, 11.15 mm; 6, 12.00 mm; 7, 5.70 mm; 8, 9.40 mm; 9, 15.00 mm; 10, 11.50 mm; 11, 5.70 mm; 12, 7.70 mm; 13, 2.35 mm; 14, 5.45 mm. (b) Configuration of the closed arrangement probe. (c) Equivalent electrical circuit.

the Nyquist plot due to micropore defects at the polymeric film surface.

The high-frequency data of the Nyquist plot corresponds to the combination of bulk resistance (R_b) and capacitance of the polymeric film−electrode system and the fitting of experimental results with the electrical equivalent circuit. Proton conductivity of the samples was calculated using the following:

$$\sigma = \frac{L}{R_b A} \tag{2}$$

where σ is the proton conductivity (S cm^{-1}), L the thickness (cm) of the polymer film, A the contact area between the electrodes and the polymer film (i.e., the electrode surface area, 1.766 cm^2), and R_b the bulk membrane resistance (Ω) calculated from the Nyquist plot.

In a second step, the ionic conductivity of membranes was determined using AC impedance spectroscopy and the through-plane conductivity method described above. For the ionic conductivity, the membranes were immersed in individual vessels containing neutral deionized water, 0.1 M NaCl, 0.1 M $NiCl_2$, and 0.1 M $CrCl_3$ aqueous solutions. In order to reach the equilibrium between the inorganic cations and the acid form of the sulfonic groups in the polymer chain, films were allowed to stabilize for 24 h. Before assays, excess surface water was removed with blotting paper and membranes were sandwiched between the contact electrodes shown in Figure 2 without any coating of silver paint. From the difference between the resistance of the blank cell (resistance of the membrane in neutral water) and the resistance with the membrane separating the working and the counter electrode compartments, the resistance of the membrane was calculated and converted to conductivity values using eq 2.

All conductivity values reported in this work correspond to the average of two membrane samples; resistances were measured at room temperature. Compression pressure was fixed at the minimal separation distance allowed by the screws used to seal the cell (Figure 2).

2.4. Electrodialysis and Polarization Curves. Following our previous study about the transport and extraction of Na^+ ions using PS/SEBS, PS/SEBS/PAni, HIPS/SEBS, and HIPS/SEBS/PAni membranes,[25] in this work we evaluate the extraction of Ni^{2+} and Cr^{3+}. Tests were conducted using a three-compartment cell described in previous studies.[31,32] Platinized titanium electrodes were used as anode and cathode. The volume in each compartment was 200 mL. Membranes were immersed in the working solutions for 48 h to reach the equilibrium state. A pseudostationary state was achieved with a pre-electrodialysis for 15 min. After this period, solutions were replaced by new ones and the experiment was restarted. Solutions of $NiCl_2$ (0.1 M) and $CrCl_3$ (0.1 M) were prepared with deionized water and poured on the working compartment cell located in the middle. Solutions of Na_2SO_4 0.1 M were poured in the compartments located on both the right and the left of the working compartment cell. The anionic membrane was the commercial Selemion AMV, which was purchased from Asahi Glass Co., while cationic membranes were those prepared in this study. The effective area of the membranes was 10 cm^2. Tests were conducted by applying a current density of 3.5 mA cm^{-2} for 4 h at 20 °C (±2 °C).

The limiting current density (i_{lim}) was derived from the variation of the membrane potential (φ_m) against the applied current density (i).[33] The $i-\varphi_m$ polarization curves were performed for all the membrane systems described above. The value of i was increased every 2 min, and the corresponding φ_m

Table 1. Chemical Composition of Polymer Films Prepared by Thermal Treatment, Sulfonation Degree (SD), Water Uptake, Ion-Exchange Capacity (IEC), Bulk Resistance (R), and Proton Conductivity (σ) Data for All Membranes Investigated in This Study

sample code	SD[a] (%)	water uptake (wt %)	IEC[b] (mequiv g^{-1})	R_b[c] (Ω)	σ[c] (S cm^{-1})	DFT[d] (μm)
PS/SEBS	13*	18*	0.86*	1.2×10^6	6.3×10^{-9}*	130 ± 11
PS/SEBS/PAni-CSA	11*	14*	1.24*	1.6×10^5	1.5×10^{-7}*	90 ± 7
PS/SEBS/PAni-DBSA	12	11	1.23	7.9×10^6	4.7×10^{-8}	70 ± 9
PS/SEBS/PAni-TSA	12	12	1.21	1.8×10^7	4.2×10^{-10}	135 ± 12
HIPS/SEBS (before annealing)	11	36	0.42	8.6×10^5	1.1×10^{-8}	156 ± 10
HIPS/SEBS (after annealing)	11*	13*	0.36*	1.8×10^7	1.6×10^{-9}*	75 ± 8
HIPS/SEBS/PAni-CSA	9*	8*	0.51*	1.4×10^6	7.1×10^{-9}*	175 ± 13
Selemion CMT	–	20	0.80	–	–	107 ± 10

[a]Measured according to the procedure indicated in the ASTM D5453-12.[26] [b]Measured by titration. [c]Measured for membranes in the dry state at room temperature, fitting the impedance data obtained to the equivalent circuit shown in Figure 2c. [d]Dry film thickness (DFT) was measured with a Neurtek Mega-Check pocket FE device. *Data taken from our previous work[25] are indicated by an asterisk.

dx.doi.org/10.1021/jp409675z | J. Phys. Chem. B 2014, 118, 1102−1112

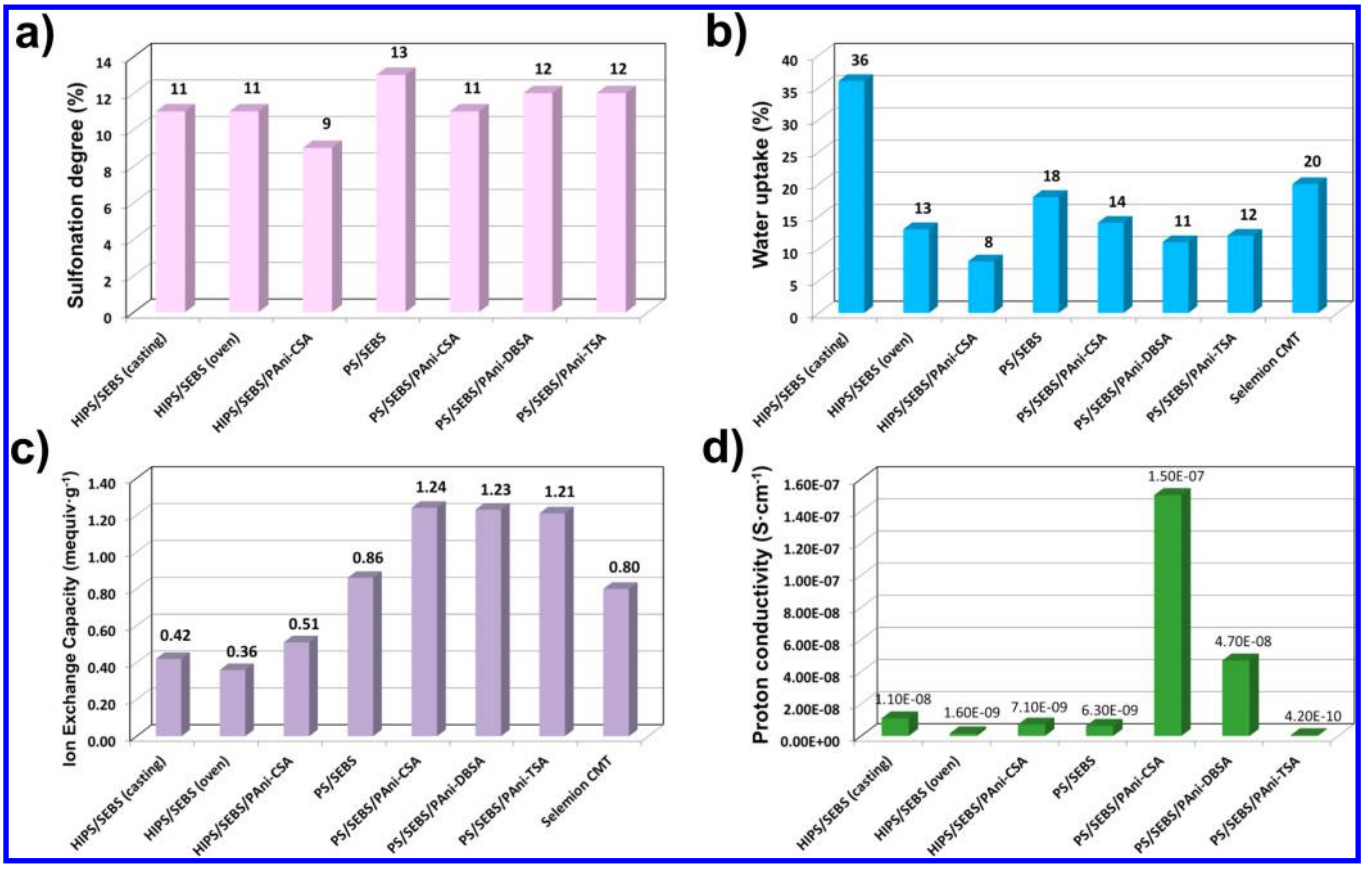

Figure 3. Correlation between the (a) sulfonation degree (SD), (b) water uptake, (c) ion-exchange capacity (IEC), and (d) proton conductivity (σ) data with the membranes investigated in this study.

was determined using two platinum contact electrodes adhered to the surface of the membrane.

All results were compared to the NaCl extraction using the three-compartment cell described in ref 25.

3. RESULTS AND DISCUSSION

3.1. Effect of Membrane Nature and the Presence of Conducting Polymers in the Proton Conductivity (Bulk Conductivity). Results reported by several groups indicate that proton conductivity increases with the sulfonation degree (SD) of PEMs[2,4,6,12] when this is achieved either by modifying the block copolymer backbone or by incorporating more polar and acid groups into the polymer chain. However, studies devoted to examining the influence of both the doped CP and the membrane preparation method on conductivity are very scarce.[31,32]

In order to correlate the conductivity with the membranes nature and their structural modification with PAni, in this work the SD concentration has been kept constant for all samples (i.e., at around 9−13%). Properties obtained for the different membranes are summarized in Table 1. The low proton conductivity achieved for all samples is in agreement with the low SD obtained using the membrane preparation described in Experimental Section. However, comparison of the conductivities obtained for doped PAni systems reveal small but non-negligible differences. Figure 3 represents the influence of the chemical nature of CEMs on their main properties. As can be seen, the proton conductivity (Figure 3a) obtained for PS/SEBS/PAni doped with CSA is 2 orders of magnitude greater (1.50×10^{-7} S cm^{-1}) than that of the polymer matrix without CP (6.3×10^{-9} S cm^{-1}). Excellent results were also previously reported for PAni-CSA conducting-isolating polymer blends compared to other dopant molecules.[25] Thus, the CSA dopant stabilizes the negative charge of the SO_3^- moiety while the influence of DBSA and TSA is reduced. Regarding the dopant structure, we assumed that the solubility of CSA into the polymer matrix is limited, leaving the SO_3^- moiety free for ion exchange with positive charges. Therefore, CSA seems to provoke some benefits in the PS/SEBS and HIPS/SEBS membranes, increasing their proton conductivity. For this reason, assays with membranes prepared by blending HIPS/SEBS with PAni-DBSA or PAni-TSA were omitted.

On the other hand, the water uptake for PS/SEBS films is close to the commercial membrane used for comparison (Selemion CMT) (Figure 3b). Indeed, the absorption of the former is higher than that of HIPS/SEBS films prepared using the same procedure (i.e., dried with thermal treatment, after annealing). The preparation method affects the porosity of the films; for this the reason, the water uptake of HIPS/SEBS membranes dried by solvent casting (36%) is greater than that of the same films dried in an oven (13%). PS/SEBS thermoplastic films have a packing density that is greater than that of HIPS/SEBS, as was evidenced by previous SEM and AFM studies.[25] Porosity has also some effect on the bulk resistance (Table 1); higher values are observed for films prepared by thermal treatment. Accordingly, films prepared by the latter procedure are less porous than those obtained by solvent casting. The only exception to this behavior corresponds to the PS/SEBS/PAni-CSA membrane, which

dx.doi.org/10.1021/jp409675z | J. Phys. Chem. B 2014, 118, 1102−1112

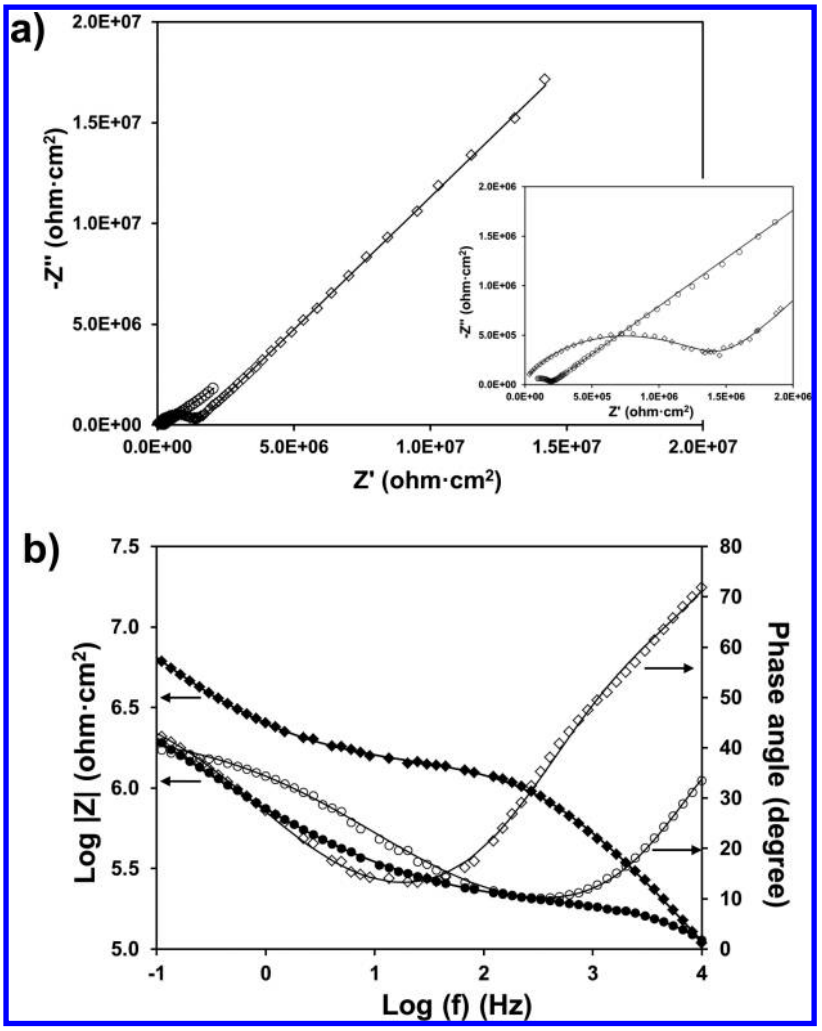

Figure 4. (a) Nyquist and (b) Bode plots of PS/SEBS (◇,◆) and PS/SEBS/PAni-CSA (○, ●) solid membrane. The inset represents a detail of the high-frequency region. Symbols are experimental vakues; lines are fitted curves.

has the lowest bulk resistance value and highest proton conductivity.

Figure 3b reveals that the incorporation of CP in the blend matrix produces a positive reduction in the water uptake, which amazingly does not affect the IEC (Figure 3c). In opposition, the IEC is higher for doped PAni-containing membranes because the CP increases the molar proportion of the amorphous phase, reducing both the crystallinity and the water uptake. On the other hand, the CP induces an inherent phase-separated morphology. This facilitates the proton transport while the low hydrophilicity of the membrane without PAni is retained.

PS/SEBS membranes, modified or not with PAni, exhibit IEC values that are more than twice that reached by HIPS/SEBS films with similar SD; in addition, the IEC of the former is higher than that of the commercial membrane used as a control. Some studies on Nafion and similar compounds attributed this behavior to the microscopic morphology after blending.[34] Commonly, the CEMs consist of two regions: (1) ionic domains formed by sulfonic groups forming hydrophilic ion clusters, which are responsible for the water uptake; and (2) a matrix formed by the polymer backbone, which corresponds to the hydrophobic region and is responsible of the mechanical integrity. However, the blends used in this work present a second ionic domain inside the membrane matrix, which is occasioned by the well-known tendency of CP molecules to agglomerate, forming clusters. Thus, doped PAni molecules provoke the apparition of new hydrophobic and hydrophilic regions in CEMs, creating new "ionic" channels. These regions maximize the proton conductivity, especially under reduced water uptake. Therefore, PAni backbone forms insoluble clusters with the polymer blend (PS/SEBS or HIPS/SEBS) and the dopant (organosulphonic acids) that in turn produce the ionic clusters, explaining the high IEC values obtained for the films with CP. To the best of our knowledge, this is an interesting observation not yet discussed in studies on CP-containing CEMs.

Results allow us to conclude that PS/SEBS presents ionic properties for use as electrodialysis membranes that are better than those of HIPS/SEBS (Figure 3d). In addition, the incorporation of a low concentration of PAni-CSA into the former improves considerably the proton conductivity in the through-plane direction. Obviously, the conductivity and IEC for the transportation and filtration of ions are expected to increase with the SD and CP concentration.

Figure 4 shows the Nyquist and Bode plots obtained for PS/SEBS and PS/SEBS/Pani-CSA membranes analyzed using the through-plane cell displayed in Figure 2. All proton conductivity values were taken from the R_b values given by the electrical circuit presented in Figure 2c (R_2) and

dx.doi.org/10.1021/jp409675z | J. Phys. Chem. B 2014, 118, 1102−1112

Table 2. Ionic Conductivity Data for Membranes Studied in This Work, after Immersion in Deionized Water, NaCl, $NiCl_2$, and $CrCl_3$ Aqueous Solutions

	ionic conductivity[a]			
solution	H_2O (S cm^{-1})	NaCl (S cm^{-1})	$NiCl_2$ (S cm^{-1})	$CrCl_3$ (S cm^{-1})
PS/SEBS	1.99×10^{-4}	4.31×10^{-5}	1.67×10^{-4}	3.09×10^{-4}
PS/SEBS/PAni-CSA	1.74×10^{-3}	2.08×10^{-3}	3.35×10^{-3}	9.03×10^{-4}
PS/SEBS/PAni-DBSA	1.65×10^{-8}	1.76×10^{-7}	5.83×10^{-4}	1.33×10^{-8}
PS/SEBS/PAni-TSA	1.02×10^{-4}	9.23×10^{-5}	3.36×10^{-8}	9.32×10^{-9}
HIPS/SEBS (before annealing)	9.03×10^{-3}	2.21×10^{-5}	1.76×10^{-5}	8.34×10^{-4}
HIPS/SEBS (after annealing)	7.68×10^{-4}	1.13×10^{-7}	9.96×10^{-5}	1.36×10^{-4}
HIPS/SEBS/PAni-CSA	2.57×10^{-4}	2.17×10^{-4}	3.14×10^{-4}	4.80×10^{-5}

[a]Measured after 24 h of immersion in the corresponding solutions, followed by superficial drying with bloting paper and at room temperature. Equivalent circuit was not possible to fit for all systems; therefore, the conductivity values are based on semicircle results obtained at high frequencies. Dry film thickness (DFT) was similar to that presented in Table 1.

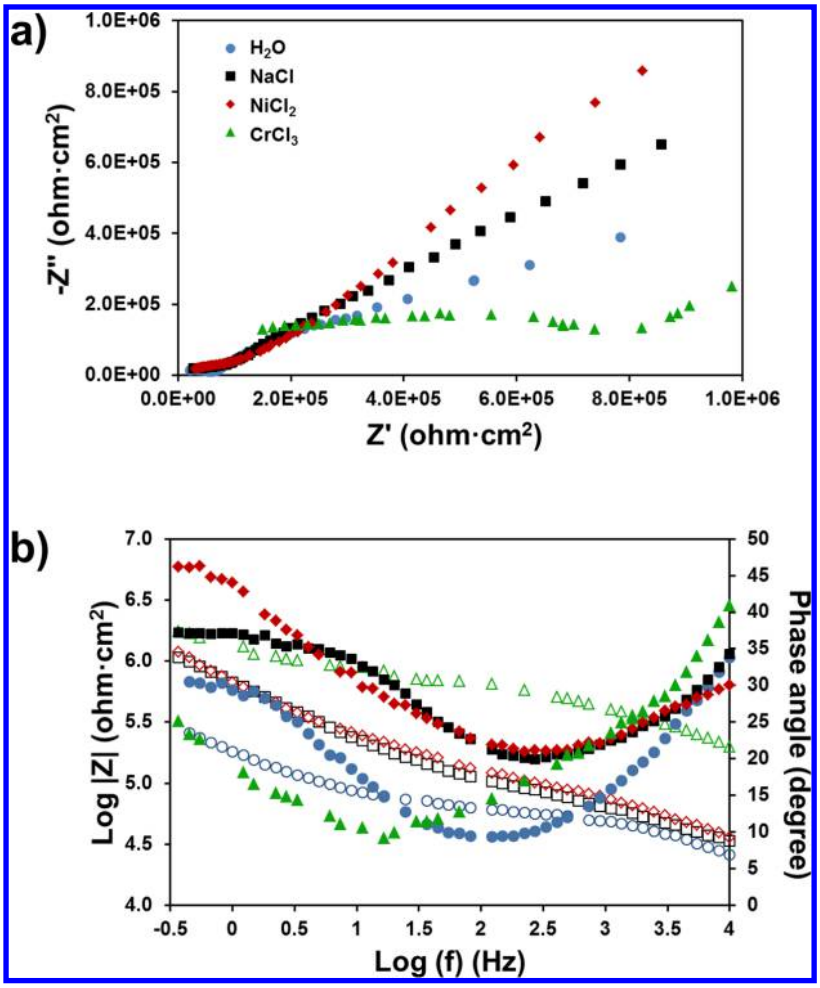

Figure 5. (a) Nyquist plot and (b) Bode plot of PS/SEBS/PAni-CSA in (●, ○) H_2O, (■, □) NaCl, (◆, ◇) $NiCl_2$, and (▲, △) $CrCl_3$ aqueous solutions. In the Bode plot, solid symbols correspond to the phase angle curves, whereas open symbols correspond to the log |Z| curves.

considering the film thickness (eq 2, Experimental Section). As we can see, the bulk membrane resistance obtained is much smaller for the film with conducting polymer (Figure 4a). The same conductivity behavior can be appreciated in the Bode plot (Figure 4b). PS/SEBS/PAni-CSA showed a maximum phase angle smaller than that of PS/SEBS sample, followed by a decrease of the overall impedance. Moreover, the time constant at high frequency shifts toward higher frequencies at the PS/SEBS/PAni-CSA sample, which can be ascribed to an increase of its conductivity. It is another parameter indicating highly efficient bulk conductivity for films containing PAni doped with CSA molecules. Other dopants tested presented bulk resistance higher than that of PS/SEBS. Indeed, TSA apparently disturbs the proton conductivity; the R_b of PS/SEBS/PAni-TSAis significantly higher than that of PS/SEBS. All the other dopants used in the present study presented bulk resistances higher than that of PS/SEBS (i.e., Nyquist and Bode plots are provided in the Supporting Information).

An important observation is that the cell arrangement used in this work has a good configuration for EIS analyses, as is

dx.doi.org/10.1021/jp409675z | J. Phys. Chem. B 2014, 118, 1102−1112

evidenced by the absence of dispersed points. Indeed, the fitted equivalent circuit shows good correlation and statistical errors between 1 and 10%. However, it should be mentioned that solid membranes in the absence of electrolyte must be painted on both sides with silver paint. If the film does not have good electrical contacts with the electrodes, the constructed cell fails and the resulting Nyquist plot is similar to that presented, as an example, in Figure S1 of the Supporting Information. Therefore, polymeric systems, isolating or conducting material, can be evaluated with the EIS technique if the cell architecture and contact electrodes are well-mounted.

Selemion CMT membrane bulk resistance and conductivity were not measured because of the presence of a plastic network inside the polymer matrix. Also, determination of the SD was not possible because of the film insolubility, which was provoked by the solid network inside the film.

3.2. Effect of Water, NaCl, $NiCl_2$, and $CrCl_3$ Permeability on Ionic Conductivity. After the bulk conductivity of the solid membranes was determined by applying the EIS technique, the film conductivity behavior in the presence of water and monovalent, divalent, and trivalent cations was examined.

Immersion of the membrane in an electrolyte provokes drastic changes in the electrical circuit because new components appear, increasing the complexity of the corresponding circuits. Considering that the EIS response at high frequencies was attributed to the membrane properties, the bulk resistance (R_b) was estimated from the first semicircle and the conductivity was calculated using eq 2. Conductivity values are given in Table 2. The area of the films was identical to that of the membranes used to determine the bulk conductivity parameters in the previous section. Accordingly, the film thickness average was assumed to be that displayed in Table 1.

Comparing the CEMs composed by PS/SEBS and modified with PAni, we verify once again that the presence of PAni-CSA inside the polymer matrix promotes the highest conductivity values with respect to other dopants, either DBSA or TSA, and with respect to the polymer without CP. In Figure 5a, we can appreciate the Nyquist plot obtained for PS/SEBS/PAni-CSA in several solutions. As we can see, the semicircle with increased diameter corresponds to the polymer film in contact with $CrCl_3$. The highest resistance obtained in $CrCl_3$ solutions is also evidenced in the Bode plot (Figure 5b) with log|Z| curve.

The diagrams for water, NaCl, and $NiCl_2$ are similar in presenting a depressed capacitive loop at higher frequency followed by a tail at lower frequencies, which can be related to diffusion processes. The bulk resistance of these three systems has the same order of magnitude. Therefore, we suppose that PS/SEBS/PAni-CSA immersed in neutral water, NaCl, and $NiCl_2$ solutions show the highest conductivity values because of easy ionic diffusion across the membrane, causing the bulk resistance decay. These results are in accordance with the electrodialysis results obtained for chromium, sodium, and nickel extraction (see Section 3.3) with this membrane.

The membrane preparation is another important factor to take into account. The EIS results obtained for HIPS/SEBS membranes in NaCl solution are shown in Figure 6. The films without further thermal treatment (HIPS/SEBS, before annealing) presented the lowest ionic conductivity because of the highest free volume inside the polymer matrix, which is responsible for high electrolyte diffusion (Figure 6). Additionally, both Nyquist curves show different behavior (Figure 6a),

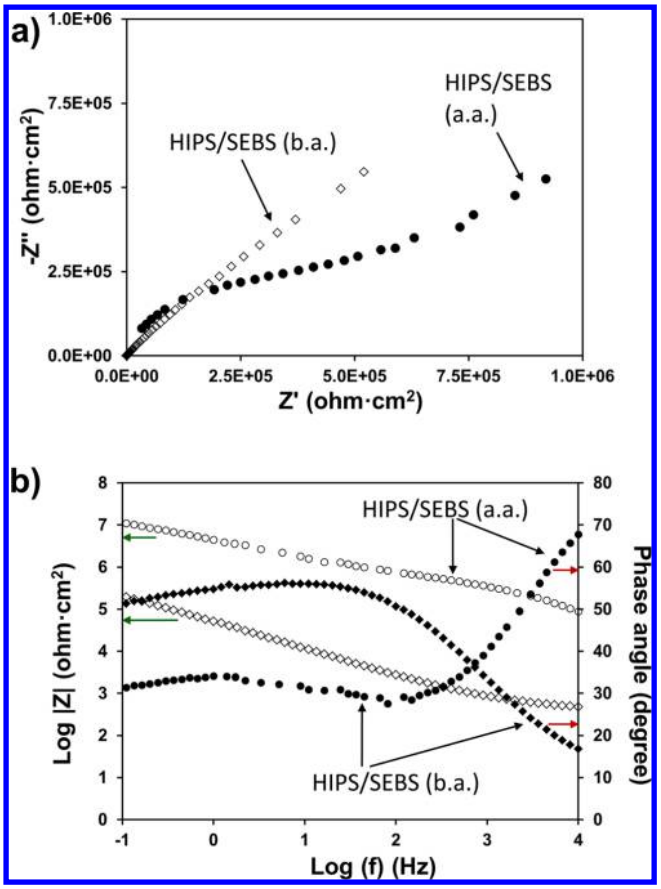

Figure 6. (a) Nyquist plot and (b) Bode plots of HIPS/SEBS films in NaCl solution, prepared by solvent casting (before annealing, b.a.) (◇, ◆) and prepared by thermal treatment (after annealing, a.a.) (○, ●).

i.e., the membrane with higher porosity presented two time constants strongly overlapped, with decreased impedance, corresponding to the ease of electrolyte diffusion across the film. On the other hand the HIPS/SEBS membrane (after annealing) shows two well-defined time constants with a capacitive loop at high frequency and a tail at lower frequencies. This observation is better seen in the Bode plot (Figure 6b), where a capacitive behavior is detected at high frequency for the HIPS/SEBS membrane (after annealing), which explains the increased bulk resistance of 2 orders of magnitude compared to the sample before annealing. Moreover, HIPS/SEBS thermoplastic films prepared by further thermal treatment have a packing density greater than that of HIPS/SEBS prepared by solvent casting; therefore, they present high isolating polymer resistance and other contributions of the ionic resistance promoted by SO_3^- groups. On the other hand, the presence of more porous material helps the polymer matrix minimize the isolating polymer resistance, increasing the number of electrolyte pathways and contributing to better ionic conductivity. The overall results allow us to conclude that CEMs without compact structures better fulfill the requirement for ion extraction, if both the mechanical integrity and the electrodialysis application lifetime are maintained. The latter aspects will be investigated in future contributions.

3.3. Comparison of Electrodialysis Results for Na^+, Ni^{2+}, and Cr^{3+} Extractions. The electrical resistance of the system during electrodialysis has been estimated using the plot of potential versus time. This potential depends on both the polymer nature and the membrane fabrication process. For

dx.doi.org/10.1021/jp409675z | J. Phys. Chem. B 2014, 118, 1102−1112

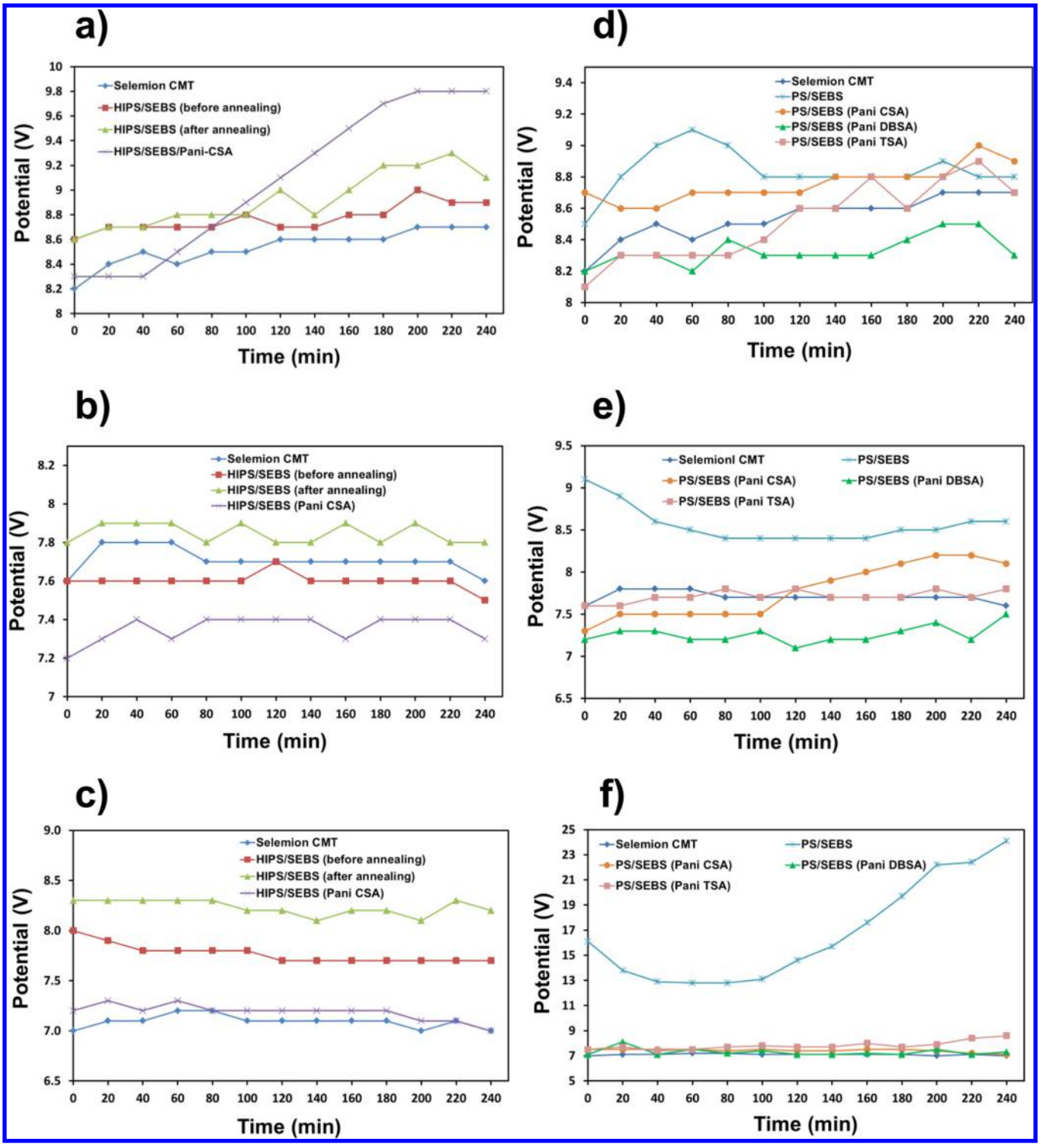

Figure 7. Potential versus time curves for the seven CEMs studied in this work: HIPS/SEBS systems (a, b, c) and PS/SEBS systems (d, e, f). Aqueous solutions: NaCl (a and d), $NiCl_2$ (b and e), and $CrCl_3$ (c and f).

example, comparison of HIPS/SEBS samples prepared by different methods (Figure 7a–c) indicates that the potential increases for the membrane with a high packing density (HIPS/SEBS after annealing) and decreases for the porous membrane (HIPS/SEBS before annealing). Indeed, HIPS/SEBS without further thermal treatment presents electrical potential stability similar to that of the commercial membrane Selemion CMT. Among HIPS/SEBS systems, the blend with PAni-CSA shows the best results for Na^+, Ni^{2+}, and Cr^{3+} electrodialysis.

The potential tends to increase with time because of the concentration reduction of the initial ionic solution (NaCl, $NiCl_2$, or $CrCl_3$). Thus, the cation migration to the cathodic compartment provokes an increment of the electric potential to keep the density current at 3.5 mA cm^{-2}. If potential remains low and stable with time and cation extraction is good, electrodialysis membranes are considered efficient in electric consumption. These conditions are successfully fulfilled by the Selemion CMT membrane, which presents a very stable

dx.doi.org/10.1021/jp409675z | J. Phys. Chem. B 2014, 118, 1102–1112

potential that increases slightly with time in the three evaluated aqueous solutions.

The PS/SEBS system seems to have potential behavior worse than that of HIPS/SEBS; the potential observed for Ni^{2+} (9.1 V) and Cr^{3+} (16.1 V) extraction are too high (Figure 7e,f). In general, the presence of CP helps the electrodialysis process, promoting the reduction of the potential with respect to the membrane without CP (Figure 7). The best potential values and stability correspond to the extraction of Cr^{3+} using PS/SEBS with doped PAni. Amazingly, the extraction percentage obtained for this trivalent cation is extremely low compared to the other cations, as is discussed below.

Results displayed in Table 3 include information about the membrane that was obtained after analysis of the compartment

Table 3. Percentage Extraction ($E_{\%}$) and Concentration ($E_{mg/L}$) of Residual Na^+, Ni^{+2}, and Cr^{3+} Ions Obtained in the Cathodic Compartment Cell after Electrodialysis Performed with the Membranes Investigated in the Present Study and Compared to Selemion CMT Commercial Membrane[a,b,c]

sample code	$E_{\%}$ Na^+	$E_{mg/L}$ Na^+	$E_{\%}$ Ni^{+2}	$E_{mg/L}$ Ni^{+2}	$E_{\%}$ Cr^{+3}	$E_{mg/L}$ Cr^{+3}
PS/SEBS	24.8[d]	519[d]	19.0	949	7.2	312
PS/SEBS/PAni-CSA	23.5[d]	510[d]	18.8	945	4.7	230
PS/SEBS/PAni-DBSA	30.6	585	6.0	278	2.3	94
PS/SEBS/PAni-TSA	21.8	469.5	17.8	901	3.2	149
HIPS/SEBS (before annealing)	21.0[d]	435[d]	16.7	893	15.0	704
HIPS/SEBS (after annealing)	20.1[d]	412[d]	16.6	878	4.8	222
HIPS/SEBS/PAni-CSA	19.9[d]	411[d]	19.8	1036	8.1	356
Selemion CMT	63.4	1242	22.8	1144	12.2	553

[a] i_{lim} = 3.5 mA cm^2. [b] Area of the membranes = 10 cm^2. [c] Electrodialysis assay performed using a three-compartment cell. [d] Data previously reported for Na^+ extraction have been included for comparison.[25]

with the filtered solution. Surprisingly, the electrical potential value or stability is not the most relevant factor for water filtration with these membranes; the most important agent is actually the film preparation method. The extraction efficiency of HIPS/SEBS before annealing is lower/higher than that of the commercial membrane for Ni^{2+} (893 and 1144 mg/L, respectively)/Cr^{3+} (704 and 553 mg/L, respectively). For Na^+ filtration, Selemion CMT is the best membrane, whereas HIPS/SEBS/PAni-CSA shows the best performance for Ni^{2+} extraction and also good behavior for Cr^{3+} extraction.

On the other hand, the extraction of metallic ions with PS/SEBS/PAni films prepared with thermal treatment is less efficient than that of corresponding membranes without CP (Table 3). Despite this unexpected result, it should be emphasized that the CP reduces the electrical resistance of the films by decreasing their electrical potential. The latter ability is particularly successful when PAni-CSA is added to PS/SEBS blends, which has been attributed to the following factors: (i) A good dispersion is achieved. (ii) The conductivity of PAni-doped CSA is higher than that obtained with other dopants. (iii) This CP stabilizes the potential−time curves registered by electrodialysis.

4. CONCLUSIONS

This work has been devoted to studying the influence of both (i) the addition of CP to blend compositions formed by triblock copolymers of SEBS and PS or HIPS and (ii) the membrane preparation method. The EIS technique has been chosen to evaluate the bulk conductivity of the membranes, which is a very important parameter for electrodialysis applications. Results allow us to conclude that cell construction is crucial in determining the conductivity parameters of the films studied here. Independent of the blend nature, the proton conductivity is promoted by the addition of CP; the best results are achieved for PAni-CSA.

HIPS/SEBS membranes have been prepared using two different procedures. Conductivity, IEC, and water uptake for films prepared by the solvent casting (HIPS/SEBS before annealing) are greater than those for films with further thermal treatment (HIPS/SEBS after annealing), which has been attributed to the low packing density of the former. Electrodialysis efficiency for HIPS/SEBS (before annealing) is also higher than that for HIPS/SEBS (after annealing). Accordingly, SEBS membranes without additional drying process show high ion diffusion, which favors cation extraction. Similar conclusions have been reached for systems in contact with water, NaCl, $NiCl_2$, or $CrCl_3$ aqueous solutions (i.e., the ionic conductivity is better in PAni-CSA-containing membranes, and films prepared by solvent casting show the highest ionic conductivity value). On the other hand, surprisingly, the presence of doped CP does not improve substantially the percentage extraction of Na^+, Ni^{2+}, or Cr^{3+} cations. Despite this, it should be noted that the CP improves the energetic consumption of the cell by reducing the electrical potential associated with the electrodialysis operation.

■ ASSOCIATED CONTENT

Supporting Information

Nyquist and Bode plots not included in the main text. This material is available free of charge via the Internet at http://pubs.acs.org.

■ AUTHOR INFORMATION

Corresponding Authors

*E-mail: elaine.armelin@upc.edu.

*E-mail: carlos.ferreira@ufrgs.br.

Notes

The authors declare no competing financial interest.

■ ACKNOWLEDGMENTS

This work has been supported by MICINN and FEDER funds (MAT2012-34498) and by the DIUE of the Generalitat de Catalunya (2009SGR925). F.M. acknowledges financial support from the CAPES agency (Grant BEX 4463/10-2) for her one-year stay at UPC. Support for the research of C.A. was received through the prize "ICREA Academia" for excellence in research (funded by the Generalitat de Catalunya).

■ REFERENCES

(1) Edmondson, C. A.; Fontanella, J. J.; Chung, S. H.; Greenbaum, S. G.; Wnek, G. E. Complex Impedance Studies of S-SEBS Block Polymer Proton-Conducting Membranes. *Electrochim. Acta* **2001**, *46*, 1623−1628.

(2) Serpico, J. M.; Ehrenberg, S. G.; Fontanella, J. J.; Jiao, X.; Perahia, D.; McGrady, K. A.; Sanders, E. H.; Kellogg, G. E.; Wnek, G. E.

Transport and Structural Studies of Sulfonated Styrene−Ethylene Copolymer Membranes. *Macromolecules* **2002**, *35*, 5916−5921.
(3) Gardner, C. L.; Anantaraman, A. V. Measurement of Membrane Conductivities Using an Open-Ended Coaxial Probe. *J. Electroanal. Chem.* **1995**, *395*, 67−73.
(4) Yang, J. E.; Lee, J. S. Selective Modification of Block Copolymers as Proton Exchange Membranes. *Electrochim. Acta* **2004**, *50*, 617−620.
(5) Kim, J.; Kim, B.; Jung, B. Proton Conductivities and Methanol Permeabilities of Membranes Made from Partially Sulfonated Polystyrene-block-poly(ethylene-ran-butylene)-block-polystyrene Copolymers. *J. Membr. Sci.* **2002**, *207*, 129−137.
(6) Wang, F.; Hickner, M.; Kim, Y. S.; Zawodzinski, T. A.; McGrath, J. E. Direct Polymerization of Sulfonated Poly(arylene ether sulfone) Random (statistical) Copolymers: Candidates for New Proton Exchange Membranes. *J. Membr. Sci.* **2002**, *197*, 231−242.
(7) He, Y.; Boswell, P. G.; Bühlmann, P.; Lodge, T. P. Ion Gels by Self-Assembly of a Triblock Copolymer in an Ionic Liquid. *J. Phys. Chem. B* **2007**, *111*, 4645−4652.
(8) Yuan, X. Z.; Song, C.; Wang, H.; Zhang, J. *Electrochemical Impedance Spectroscopy in Proton Exchange Membrane Fuel Cells. Fundamentals and Applications*, 1st. ed.; Springer-Verlag: London, 2010.
(9) Park, C. H.; Leeb, C. H.; Guiver, M. D.; Lee, Y. M. Sulfonated Hydrocarbon Membranes for Medium-Temperature and Low-Humidity Proton Exchange Membrane Fuel Cells (PEMFCs). *Prog. Polym. Sci.* **2011**, *36*, 1443−1498.
(10) Soboleva, T.; Xie, Z.; Shi, Z.; Tsang, E.; Navessin, T.; Holdcroft, S. Investigation of the Through-Plane Impedance Technique for Evaluation of Anisotropy of Proton Conducting Polymer Membranes. *J. Electroanal. Chem.* **2008**, *622*, 145−152.
(11) Mistry, M. K.; Choudhury, N. R.; Dutta, N. K.; Knott, R. Inorganic Modification of Block Copolymer for Medium Temperature Proton Exchange Membrane Application. *J. Membr. Sci.* **2010**, *351*, 168−177.
(12) Shi, Z.; Holdcroft, S. Synthesis and Proton Conductivity of Partially Sulfonated Poly([vinylidene difluoride-co-hexafluoropropylene]-*b*-styrene) Block Copolymers. *Macromolecules* **2005**, *38*, 4193−4201.
(13) Tsang, E. M. W.; Zhang, Z.; Yang, A. C. C.; Shi, Z.; Peckham, T. J.; Narimani, R.; Frisken, B. J.; Holdcroft, S. Nanostructure, Morphology, and Properties of Fluorous Copolymers Bearing Ionic Grafts. *Macromolecules* **2009**, *42*, 9467−9480.
(14) Lee, W. J.; Jung, H. R.; Lee, M. S.; Kim, J. H.; Yang, K. S. Preparation and Ionic Conductivity of Sulfonated-SEBS/SiO_2/plasticizer Composite Polymer Electrolyte for Polymer Battery. *Solid State Ionics* **2003**, *164*, 65−72.
(15) Mokrini, A.; Huneault, M. A.; Shi, Z.; Xie, Z.; Holdcroft, S. Non-fluorinated Proton-exchange Membranes Based on Melt Extruded SEBS/HDPE Blends. *J. Membr. Sci.* **2008**, *325*, 749−757.
(16) Gardner, C. L.; Anantaraman, A. V. Studies on Ion-exchange Membranes. II. Measurement of Anisotropic Conductance of Nafion®. *J. Electroanal. Chem.* **1998**, *449*, 209−214.
(17) Ma, S.; Siroma, Z.; Tanaka, H. Anisotropic Conductivity Over In-Plane and Thickness Directions in Nafion-117. *J. Electrochem. Soc.* **2006**, *153*, A2274−A2281.
(18) Blachot, J. F.; Diat, O.; Putaux, J. L.; Rollet, A. L.; Rubatat, L.; Vallois, C.; Muller, M.; Gebel, G. Anisotropy of Structure and Transport Properties in Sulfonated Polyimide Membranes. *J. Membr. Sci.* **2003**, *214*, 31−42.
(19) Parthasarathy, A.; Dave, B.; Srinivasan, S.; Appleby, A. J.; Martin, C. R. The Platinum Microelectrode/Nafion Interface: An Electrochemical Impedance Spectroscopic Analysis of Oxygen Reduction Kinetics and Nafion Characteristics. *J. Electrochem. Soc.* **1992**, *139*, 1634−1641.
(20) Wu, G. M.; Lin, S. J.; Yang, C. C. Preparation and Characterization of High Ionic Conducting Alkaline Non-woven Membranes by Sulfonation. *J. Membr. Sci.* **2006**, *284*, 120−127.
(21) Wang, J. C. Model for Impedance of a Solid Ionic Conductor Sandwiched between Blocking Electrodes. *Electrochim. Acta* **1993**, *38*, 2111−2114.
(22) Yang, C. C.; Lin, S. J. Alkaline Composite PEO−PVA−glass-fibre-mat Polymer Electrolyte for Zn−air Battery. *J. Power Sources* **2002**, *112*, 497.
(23) Wu, G. M.; Lin, S. J.; Yang, C. C. Preparation and characterization of PVA/PAA membranes for solid polymer electrolytes. *J. Membr. Sci.* **2006**, *275*, 127−133.
(24) Wintersgill, M. C.; Fontanella, J. J. Complex Impedance Measurements on Nafion. *Electrochim. Acta* **1998**, *43*, 1533−1538.
(25) Müller, F.; Ferreira, C. A.; Franco, L.; Puiggalí, J.; Alemán, C.; Armelin, E. New Sulfonated Polystyrene and Styrene−Ethylene/Butylene−Styrene Block Copolymers for Applications in Electrodialysis. *J. Phys. Chem. B* **2012**, *116*, 11767−11779.
(26) *Standard Test Method for Determination of Total Sulfur in Light Hydrocarbons, Spark Ignition Engine Fuel, Diesel Engine Fuel, and Engine Oil by Ultraviolet Fluorescence*; ASTM D5453. ASTM International, 2012.
(27) Prakash, S.; Sivakumar, C.; Rajendran, V.; Vasudevan, T.; Gopalan, A.; Wen, T. C. Growth Behavior of Poly(*o*-toluidine-co-*p*-fluoroaniline) Deposition by Cyclic Voltammetry. *Mater. Chem. Phys.* **2002**, *74*, 74−82.
(28) Wang, M.; Zhao, F.; Guo, Z.; Dong, S. Poly(vinylidene fluoride-hexafluoropropylene)/organo-montmorillonite Clays Nanocomposite Lithium Polymer Electrolytes. *Electrochim. Acta* **2004**, *49*, 3595−3602.
(29) Wang, M.; Zhao, F.; Dong, S. A Single Ionic Conductor Based on Nafion and Its Electrochemical Properties Used As Lithium Polymer Electrolyte. *J. Phys. Chem. B* **2004**, *108*, 1365−1370.
(30) Rodrigues, I. R.; Forte, M. M. C.; Azambuja, D. S.; Castagno, K. R. L. Synthesis and Characterization of Hybrid Polymeric Networks (HPN) Based on Polyvinyl Alcohol/chitosan. *React. Funct. Polym.* **2007**, *67*, 708−715.
(31) Amado, F. D. R.; Gondran, E.; Ferreira, J. Z.; Rodrigues, M. A. S.; Ferreira, C. A. Synthesis and Characterisation of High Impact Polystyrene/polyaniline Composite Membranes for Electrodialysis. *J. Membr. Sci.* **2004**, *234*, 139−145.
(32) Amado, F. D. R.; Rodrigues, L. F., Jr.; Rodrigues, M. A. S.; Bernardes, A. M.; Ferreira, J. Z.; Ferreira, C. A. Development of Polyurethane/polyaniline Membranes for Zinc Recovery through Electrodialysis. *Desalination* **2005**, *186*, 199−206.
(33) Tanaka, Y. Concentration Polarization in Ion-Exchange Membrane Electrodialysis: The Events Arising in a Flowing Solution in a Desalting Cell. *J. Membr. Sci.* **2003**, *216*, 149−164.
(34) Weissbach, T.; Tsang, E. M. W.; Yang, A. C. C.; Narimani, R.; Frisken, B. J.; Holdcroft, S. Structural Effects on the Nano-Scale Morphology and Conductivity of Ionomer Blends. *J. Mater. Chem.* **2012**, *22*, 24348−24355.

Supporting Information

Measuring the Proton Conductivity of Ion-Exchange Membranes Using EIS Technique and a Through-Plane Cell

Franciélli Müller,[1] Carlos A. Ferreira,[1*] Denise S. Azambuja,[2] Carlos Alemán,[3,4] Elaine Armelin,[3,4*]

[1] Departamento de Engenharia de Materiais, PPGEM, Universidade Federal do Rio Grande do Sul, Av. Bento Gonçalvez, 9500, Setor 4, Prédio 74- 91501-970, Porto Alegre (RS), Brazil.

[2] Instituto de Química, Universidade Federal do Rio Grande do Sul, Av. Bento Gonçalves 9500 – CEP 91501-970, Porto Alegre (RS), Brazil

[3] Departament d'Enginyeria Química, ETSEIB, Universitat Politècnica de Catalunya, Av. Diagonal 647, 08028, Barcelona, Spain.

[4] Centre for Research in Nano-Engineering, Universitat Politècnica de Catalunya, Campus Sud, Edifici C', C/Pasqual i Vila s/n, 08028, Barcelona, Spain

Corresponding Authors: elaine.armelin@upc.edu and carlos.ferreira@ufrgs.br

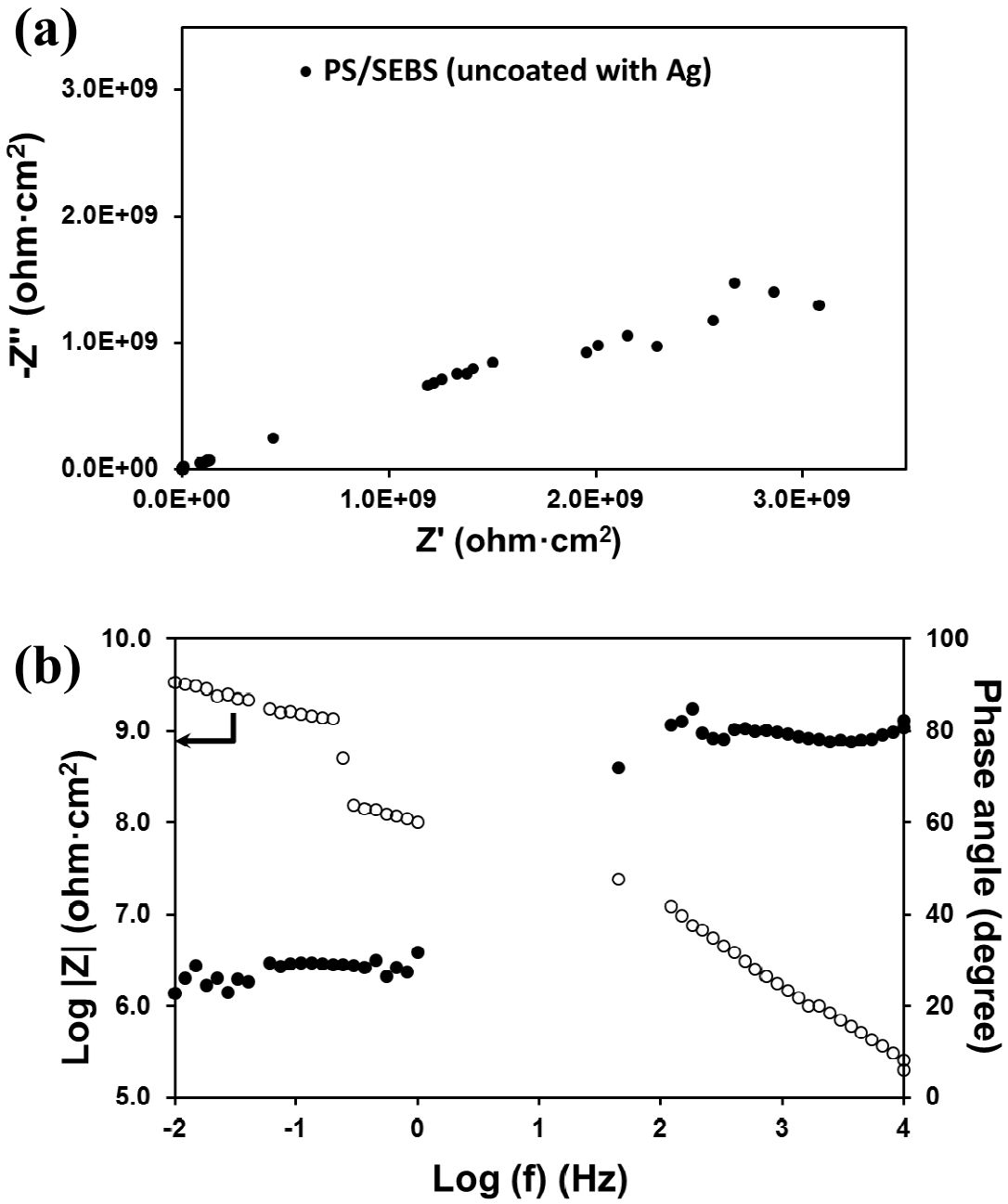

Figure S1. Example of Nyquist plot (a) and Bode plot (b) of a dry membrane without good electrical contact and in the through-plane cell.

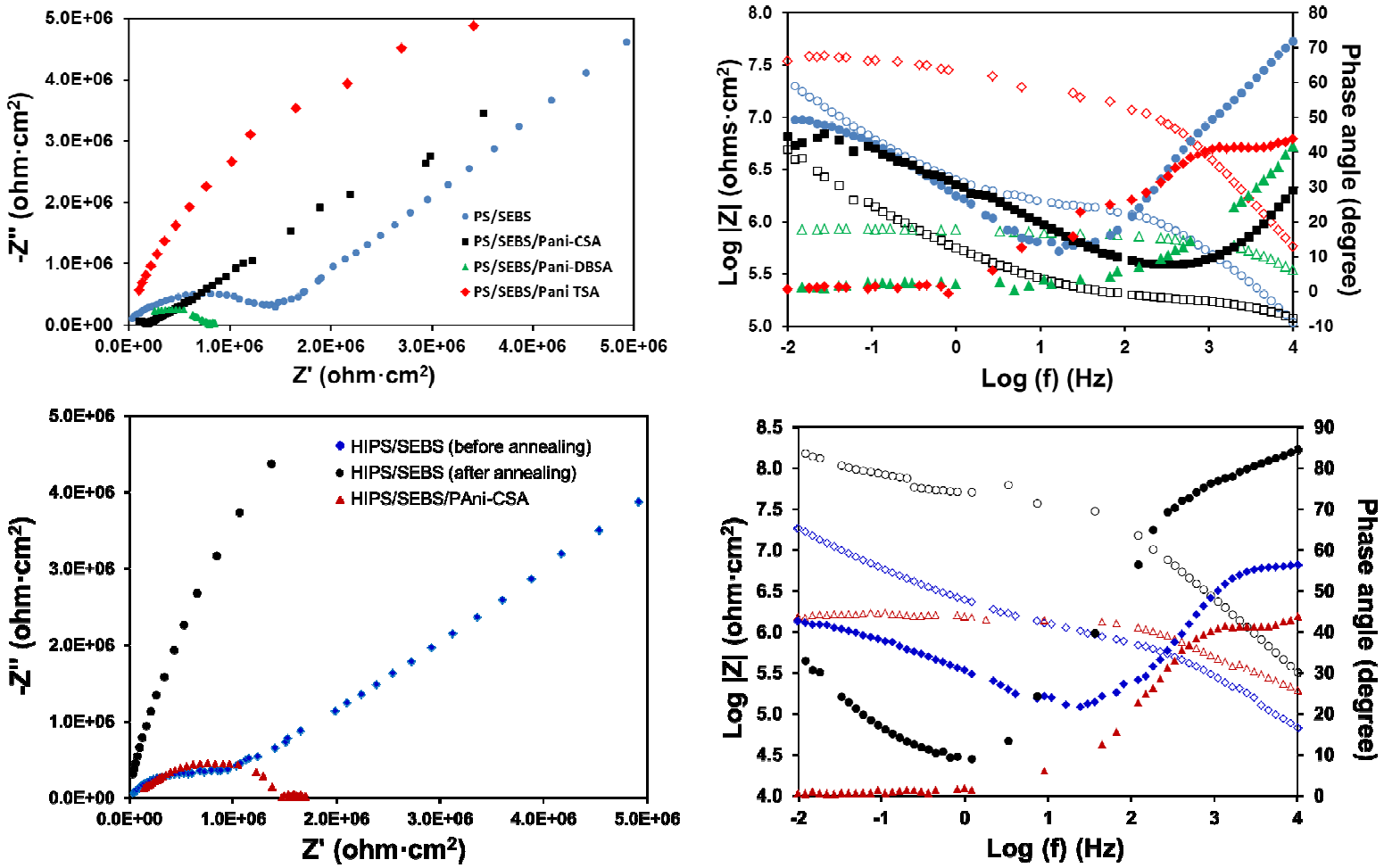

Figure S2. Nyquist (left) and Bode plots (right) obtained for the dried PS/SEBS (top) and HIPS/SEBS (botton) membranes used to measure the bulk resistance. The legend for Bode curves are the same that showed for Nyquist plot, where solid symbols regards Phase angle axis and empty symbols regards Log |Z| axis.

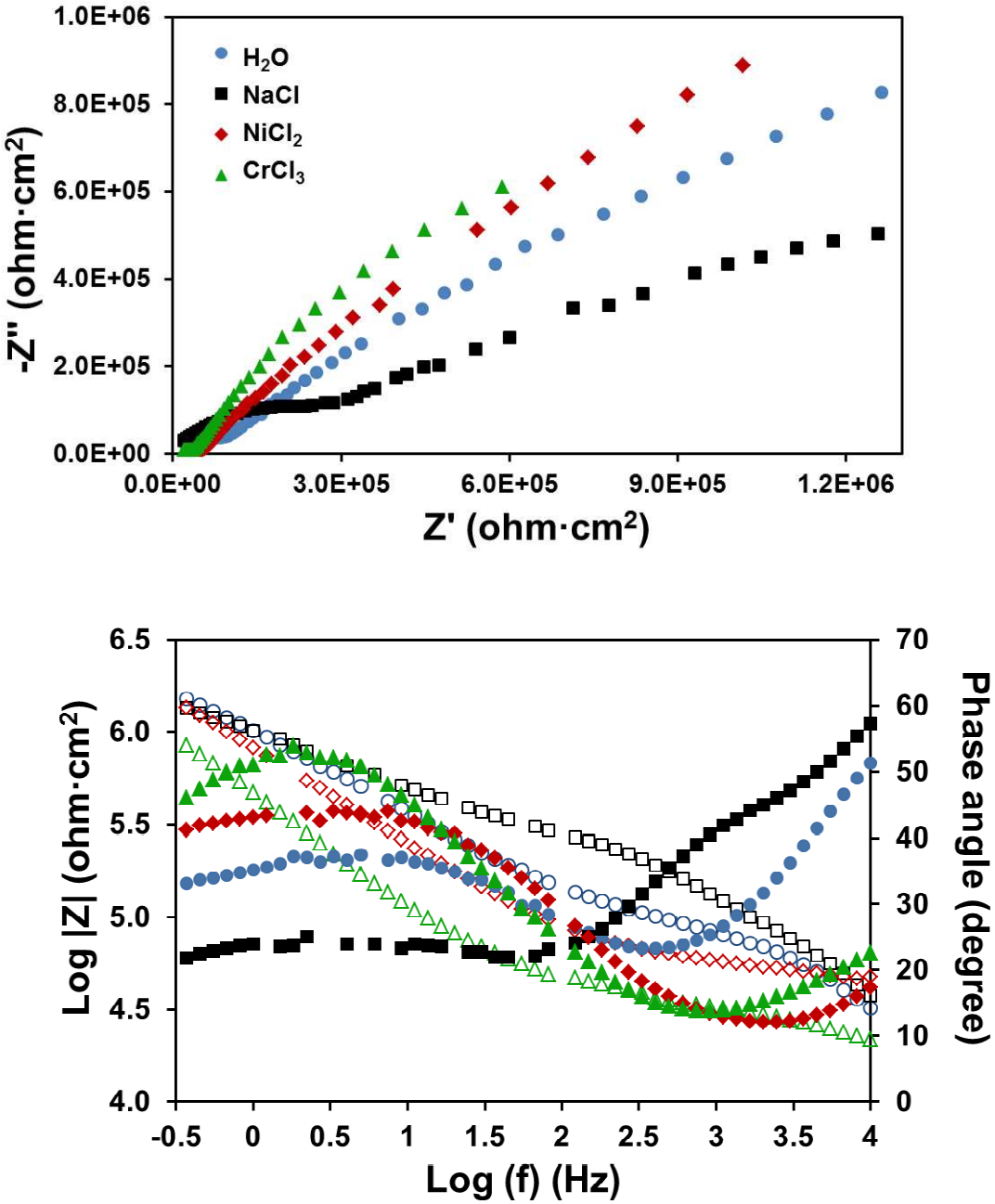

Figure S3. Nyquist (top) and Bode plots (bottom) of PS/SEBS membranes after immersion in several solutions. The legend for Bode curves are the same that showed for Nyquist plot, where solid symbols regards Phase angle axis and empty symbols regards Log |Z| axis.

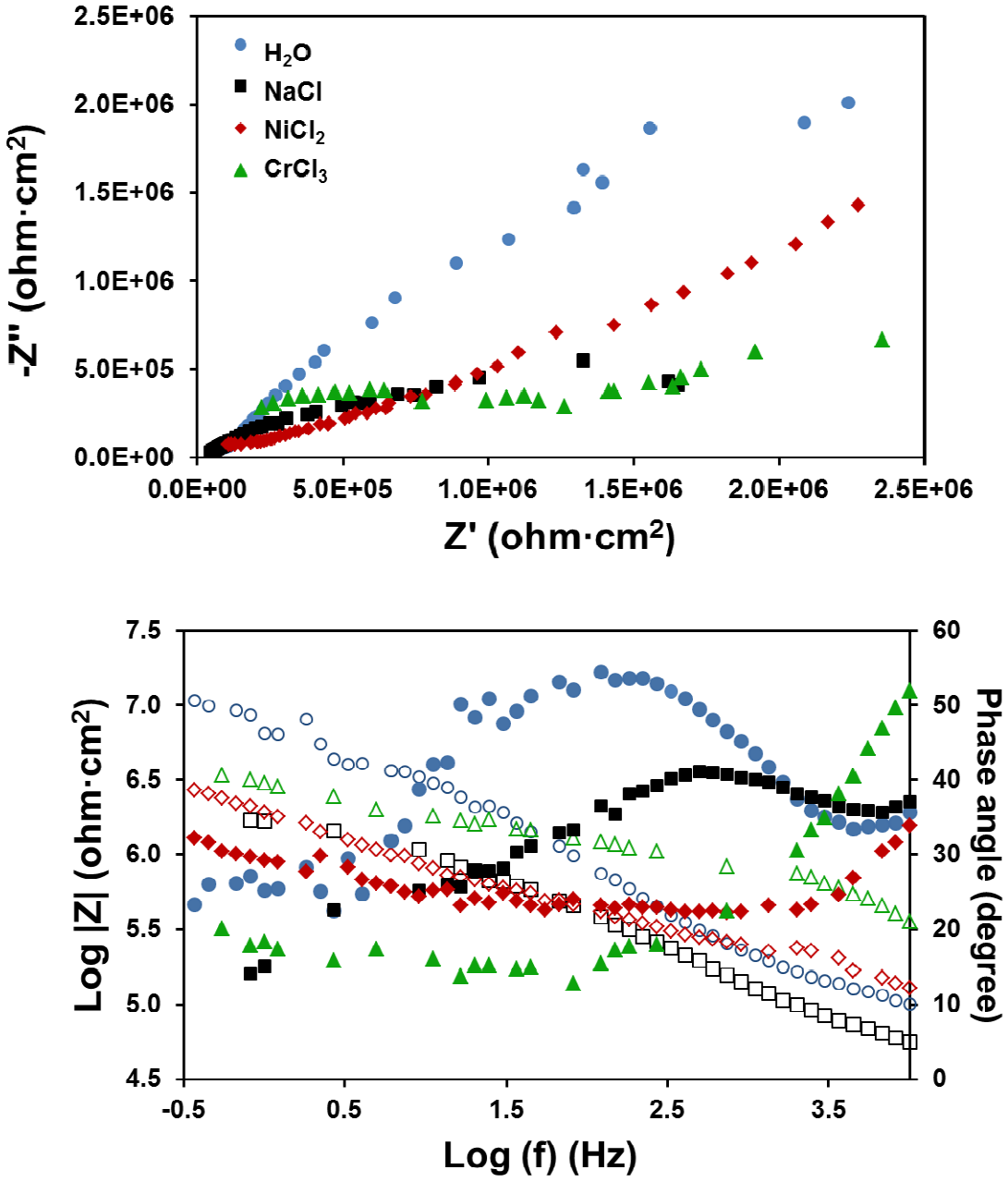

Figure S4. Nyquist (top) and Bode plots (bottom) of PS/SEBS/PAni-DBSA membranes after immersion in several solutions. The legend for Bode curves are the same that showed for Nyquist plot, where solid symbols regards Phase angle axis and empty symbols regards Log |Z| axis.

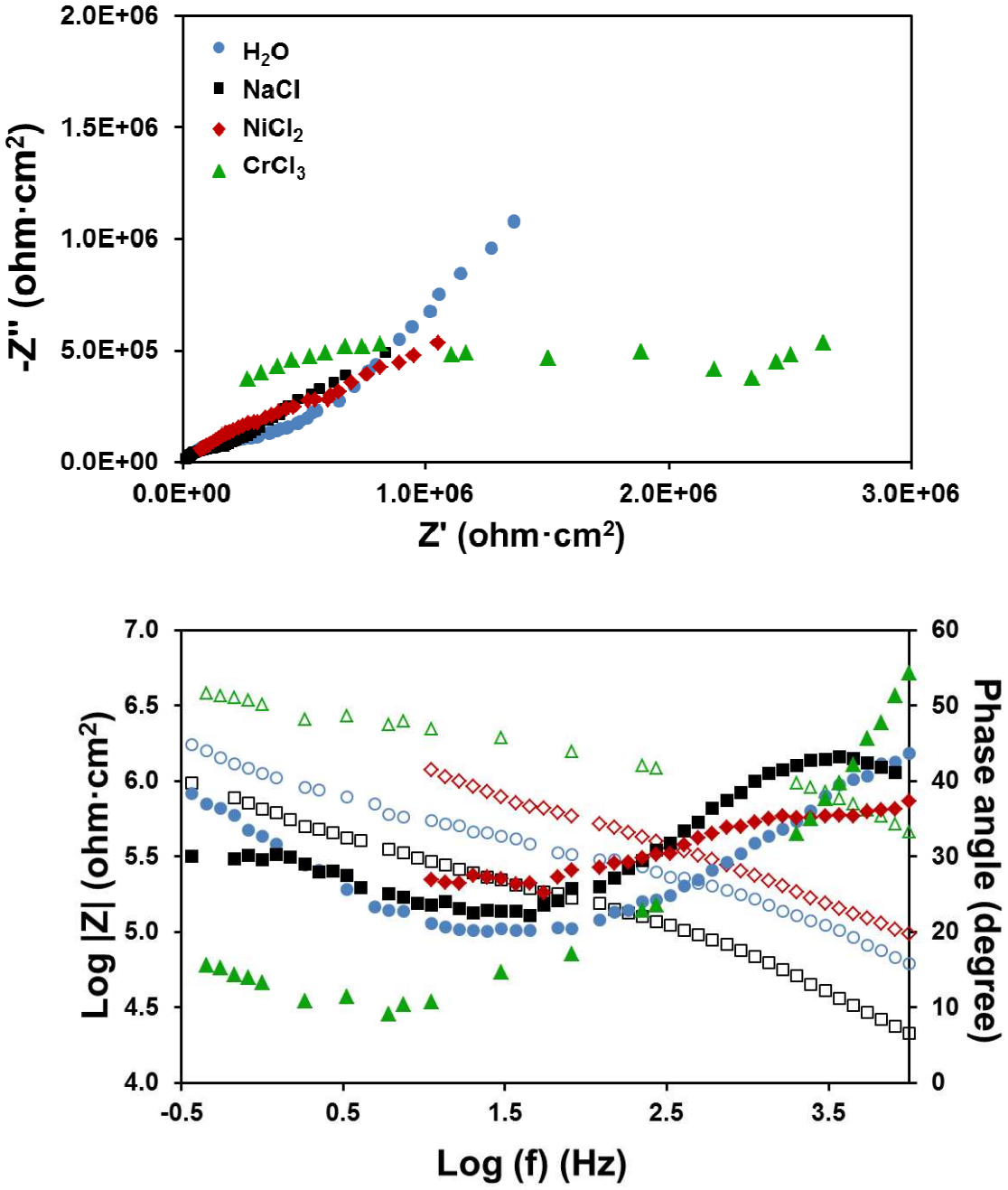

Figure S5. Nyquist (top) and Bode plots (bottom) of PS/SEBS/PAni-TSA membranes after immersion in several solutions. The legend for Bode curves are the same that showed for Nyquist plot, where solid symbols regards Phase angle axis and empty symbols regards Log |Z| axis.

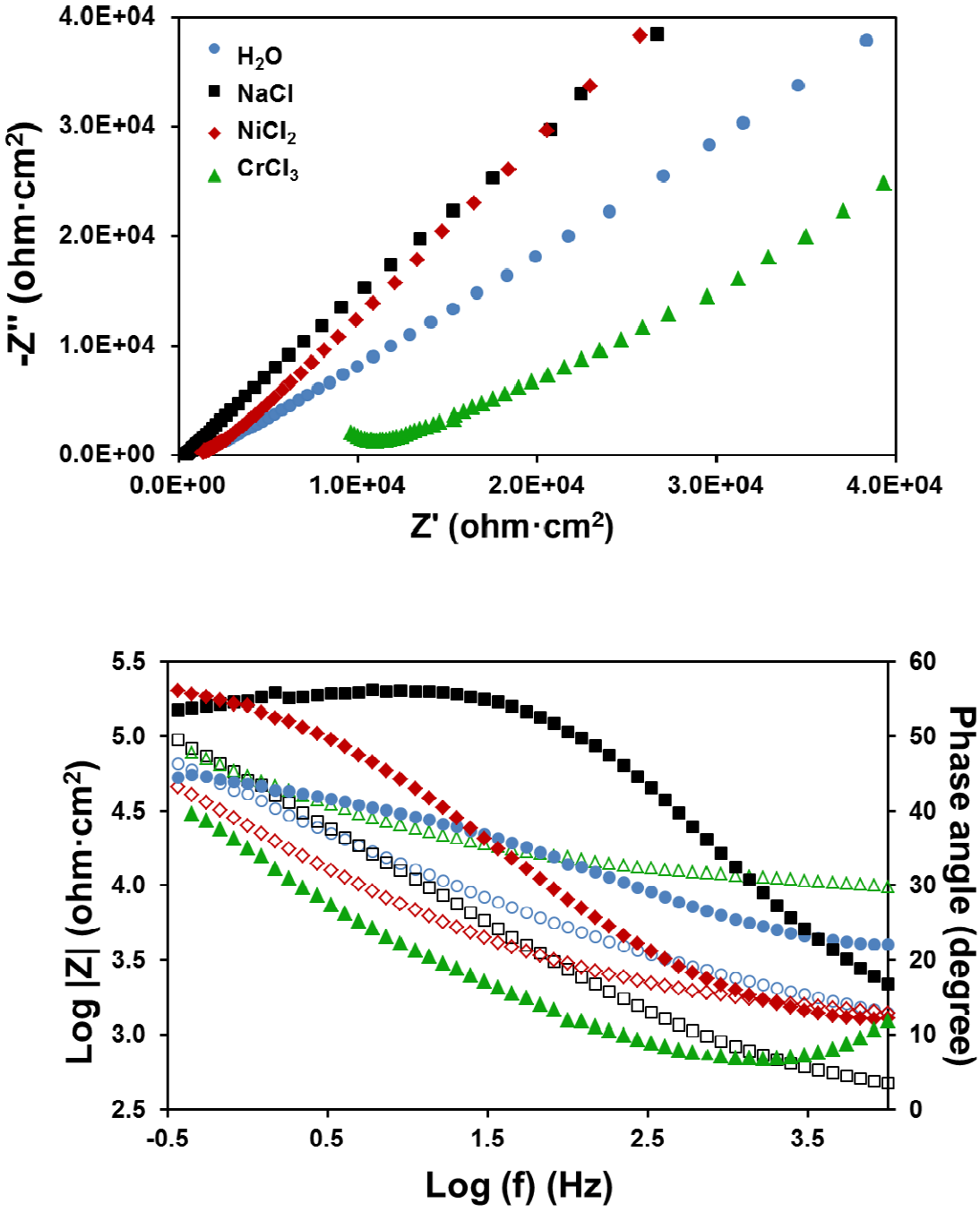

Figure S6. Nyquist (top) and Bode plots (bottom) of HIPS/SEBS (before annealing) membranes after immersion in several solutions. The legend for Bode curves are the same that showed for Nyquist plot, where solid symbols regards Phase angle axis and empty symbols regards Log |Z| axis.

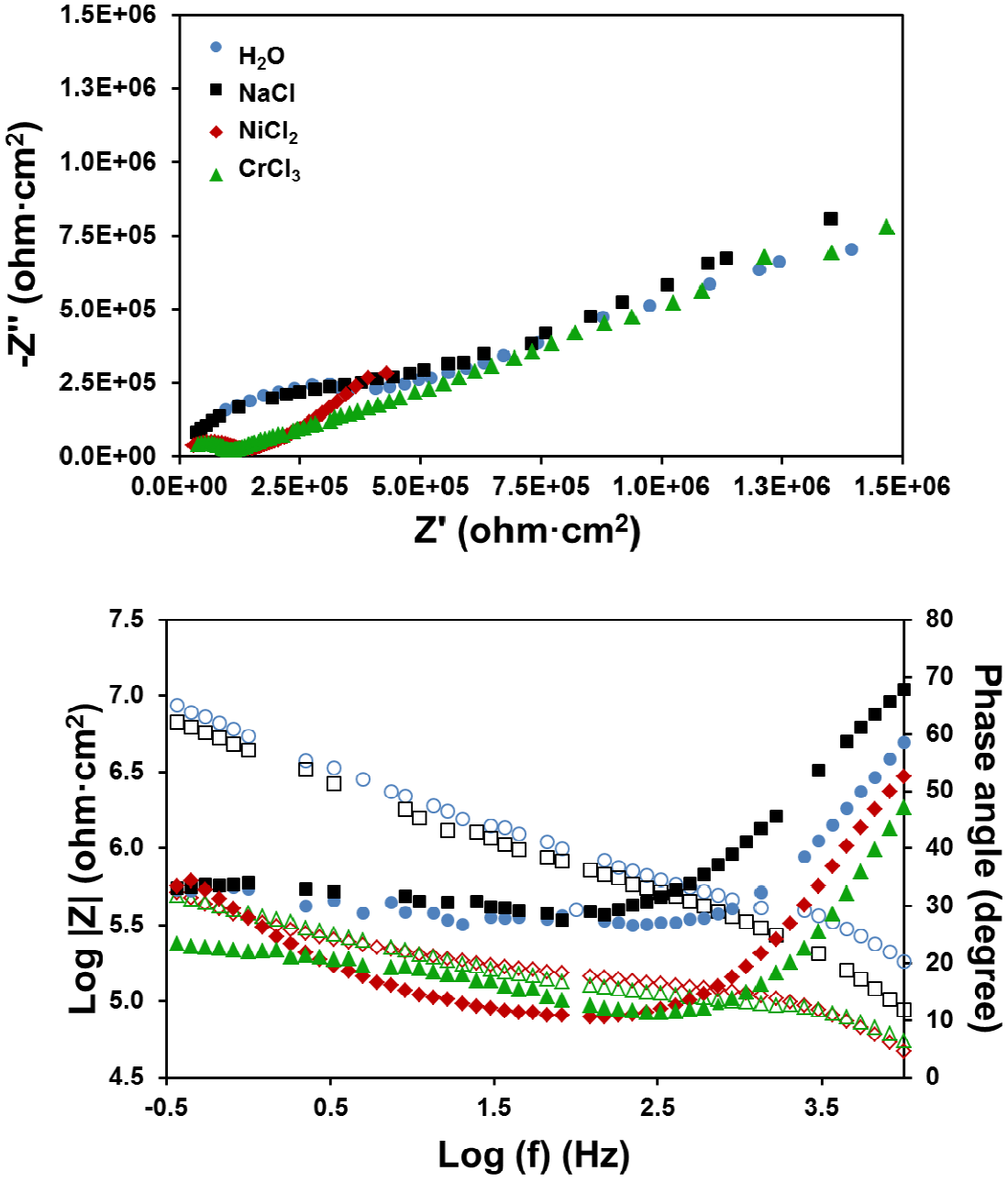

Figure S7. Nyquist (top) and Bode plots (bottom) of HIPS/SEBS (after annealing) membranes after immersion in several solutions. The legend for Bode curves are the same that showed for Nyquist plot, where solid symbols regards Phase angle axis and empty symbols regards Log |Z| axis.

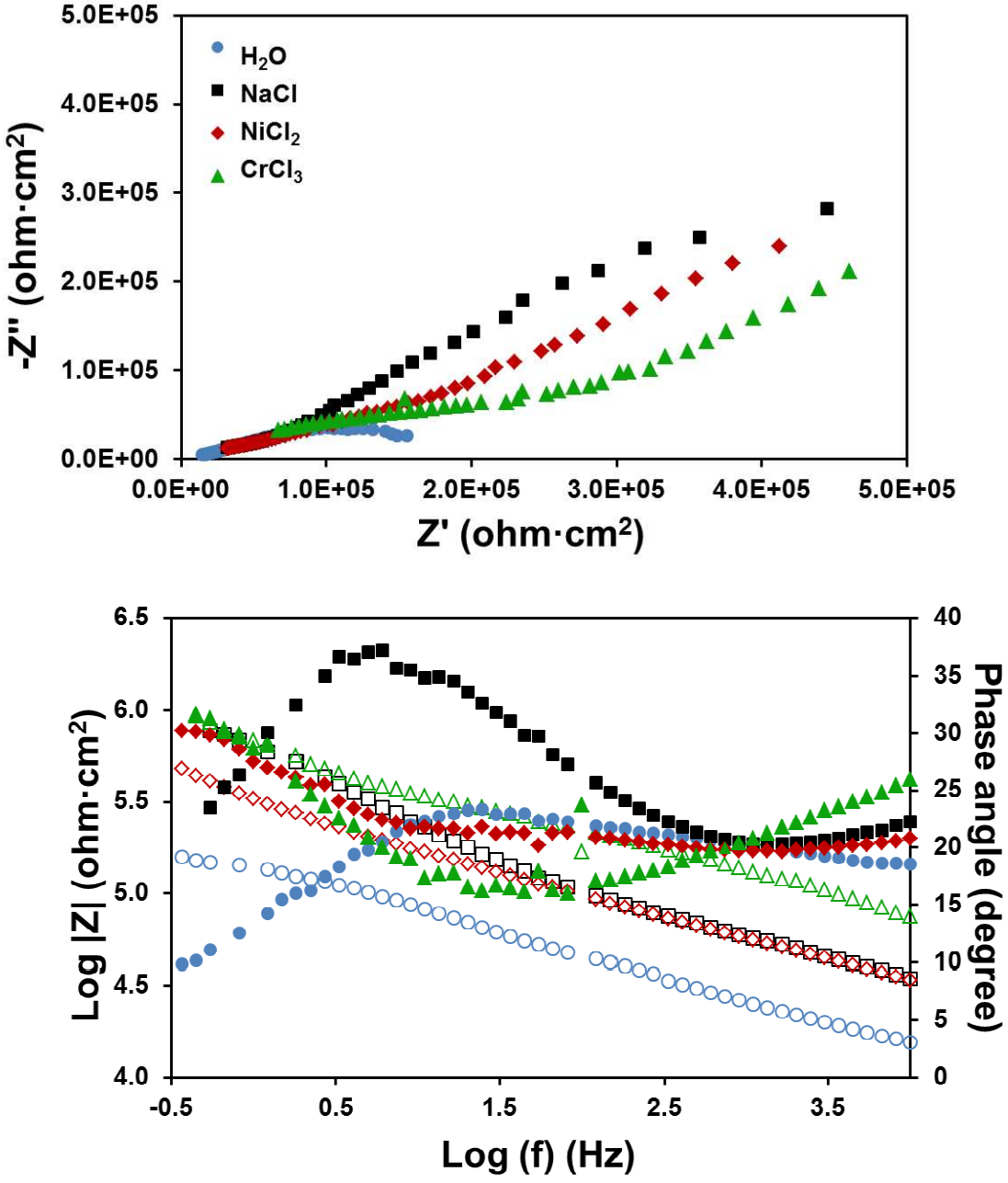

Figure S8. Nyquist (top) and Bode plots (bottom) of HIPS/SEBS/PAni-CSA membranes after immersion in several solutions. The legend for Bode curves are the same that showed for Nyquist plot, where solid symbols regards Phase angle axis and empty symbols regards Log |Z| axis.